COVER SHEET

Paper Number: **342**

Title: **In-Plane Shear Response of GFRP Laminates by ± 45° and 10° Off-axis Tensile Testing using Digital Image Correlation[1]**

Authors: Matthias Merzkirch
            Qi An
             Aaron M. Forster

ABSTRACT

For the determination of the shear strength, strain and modulus of reinforced composites, nearly a dozen measurement techniques exist, several of which are supported by ASTM or ISO standards. One reason for so many options is the difficulty in obtaining a reasonably pure and uniform shear stress state in the test specimen.

Typically, linear strain gauges and rosette strain gauges have been used to measure deformations for the determination of the elastic modulus and the strain to failure in many of these methods. The advent of optical strain measurement techniques such as digital image correlation (DIC), provide new opportunities to generate high resolution maps of the shear strain field as a function of the globally applied strain. DIC allows for the full-field mapping of the deformations (in-plane and out-of-plane for stereo DIC) and strains (normal and shear), revealing the pattern of deformation and damage throughout the specimen. In this work, it is shown that non-contact measurements of the strain field are an important enhancement to measuring the shear properties of fiber reinforced polymer (FRP) composites.

This contribution describes the use of DIC for the shear strain response while performing standardized bias extension tests on ± 45° layups and non-standardized 10° off-axis tensile tests on glass fiber reinforced (GFRP) coupon specimens. Shear moduli and shear strengths obtained will be compared to results using the V-notched method.

_____

Matthias Merzkirch, Guest Researcher, Materials Science and Engineering Division, Material Measurement Laboratory, National Institute of Standards and Technology, Gaithersburg, MD 20899 USA

Qi An, Theiss Research, La Jolla, CA, 92037, USA; Materials Measurement Science Division, Material Measurement Laboratory, National Institute of Standards and Technology, Gaithersburg, MD 20899 USA

Aaron M. Forster, Materials Measurement Science Division, Material Measurement Laboratory, National Institute of Standards and Technology, Gaithersburg, MD 20899 USA

INTRODUCTION

The accurate measurement of modulus and strength properties in tension, compression and shear is the first step in the design of fiber reinforced polymer (FRP) composite materials. There are many different shear test methods (> 10 methods) for unidirectional and quasi-isotropic fiber reinforced composites. Each shear test method has its benefits, constraints and limitations, with some more appropriate for interlaminar (through thickness) shear properties and others appropriate for intralaminar (in-plane) shear properties. One reason for so many choices is the difficulty in obtaining a reasonably pure and uniform shear stress state in the test specimen, which is critical if true shear properties are to be measured. The short beam strength test (ASTM D2344) [1] is a popular method for screening the apparent interlaminar strength of fiber composites. Another method that is not used as frequently include the double-notch shear test (ASTM D3846) [2]. Unfortunately, neither standard provides an accurate measure of interlaminar stiffness. In Merzkirch et al. [3], digital image correlation (DIC) was used to determine the interlaminar shear modulus during three-point and four-point flexural tests. For the determination of the in-plane shear properties for certain fiber orientations, the V-notched beam test ('Iosipescu', ASTM D5379) [4] and V-Notched rail shear test (ASTM D7078) [5] use a "butterfly" shaped specimen.

In this work, the standardized $\pm 45°$ bias extension test [6] [7] [8] and the non-standardized 10° off-axis tensile test [9] [10] were chosen to measure a low density (LD) E-glass fabric epoxy-based composites. Distributions of shear strains were analyzed using digital image correlation [11]. DIC is a topological non-contact material independent solution for full field determination of displacements, deformation and strain. We provide an analysis of how optical strain methods are important for FRP material shear testing by comparing tensile test responses from FRP composite materials in terms of shear strength, shear modulus, and shear strain distributions.

EXPERIMENTAL

Materials and Composites Manufacturing

A low density (LD) E-glass unidirectional (UD) fabric (Style 7721, Thayercraft Inc., USA) [2] was used to make glass fiber-reinforced polymer (GFRP) composites. Approximately 15 % of the overall fabric mass are the stitching fibers, which are aligned perpendicular to the UD fibers. These stitching fibers are the same E-glass materials woven but have a lower density than the UD fibers. The nominal fabric density was approximately 2.03 g/cm^3. Four plies of the as-received, LD E-glass UD fabric were infused with a stoichiometric ratio of EPON 862 and Epi-Kure W (Hexion Specialty Chemicals) using a vacuum-assisted resin transfer molding process (VARTM). The UD fibers were oriented according to the fiber orientation 0º, 90º, or ± 45º. Distribution media was applied to aid the through-thickness resin infusion. The double bag technique

---

[2] Certain commercial equipment, instruments, or materials are identified in this paper in order to specify the experimental procedure adequately. Such identification is not intended to imply recommendation or endorsement by the National Institute of Standards and Technology, nor is it intended to imply that the materials or equipment identified are necessarily the best available for the purpose.

was utilized to facilitate a uniform infusion surface and reduce final part (plaque) thickness variability. The infusion of the vacuum-degassed resin occurred under vacuum (nominally -100 kPa) and at about 55 °C using a flow media to aid through-thickness resin diffusion. Infusion took place over approximately 0.5 h before the final cure under vacuum at about130 °C for approximately 6 h [12] [13]. The plaques had a length of about 35 cm, a width of around 25 cm, a nominal thickness of 0.93 mm and a reinforcing fiber fraction of $(54.31 \pm 0.35)\%$ by mass. The reinforcing fraction was determined through thermal gravimetric measurements of five plaques. The $\pm$ 45° plaque was a non-symmetric layup [+ 45, - 45, + 45, - 45] which leads to a monoclastic curvature in the plaque, see Figure 1a (back).
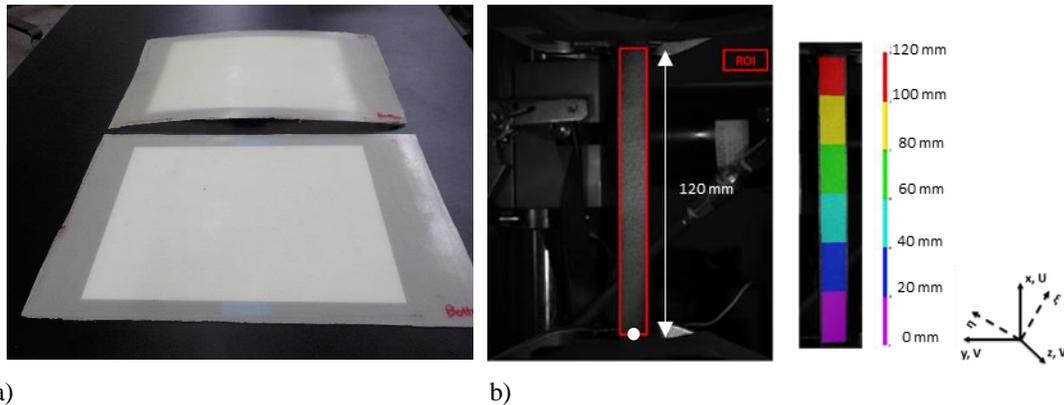
Figure 1: a) Plaques $\pm$ 45° (back), UD (front) b) Field of View (FOV) and Region of interest (ROI), colored area (right) from rectangular specimens cut from the plaques. The white dot in b) indicates the location of the origin.

Tensile-Testing Setup and DIC Configuration

The $\pm$ 45° specimens were cut with a waterjet system to a nominal width of $w = 25$ mm, a total length of about 268 mm resulting in a gauge length of $l \approx 140$ mm and an aspect ratio of 5.6. The 10° specimens have been cut to a nominal width of $w = 13$ mm, a total length of about 210 mm resulting in a gauge length of $l \approx 125$ mm and an aspect ratio of 9.6. Tabs with a length of about 42 mm were used for the 10° specimens only. Further details about specimen preparation can be found in [14].

The displacement-controlled tests ($N = 2$ per material configuration) were conducted on a servo hydraulic testing machine at a nominal rate of 0.0001 s^{-1}. The loading was induced by the actuator located at the bottom of the test frame. The specimens were rigidly gripped with anti-rotation collars having diamond jaw surfaces. A clamping pressure of approximately 5 MPa was used for a specimen width of nominally 25 mm and approximately 4 MPa for a specimen width of nominally 13 mm. Further details about the testing setup can be found in [14]. All specimens were prepared for DIC measurement by spraying first with commercially available matte white spray paint, which was applied directly onto the specimen, and, after drying, by applying matte black spray paint with an intended overspray to create a random speckle pattern. For stereo-DIC measurement, two 4.2 megapixel (MP) (2048 pixel x 2048 pixel) charge-coupled device (CCD) cameras and 35 mm fixed focal length lenses were used. For data acquisition and analysis, a commercially available DIC software package was

used. The image acquisition rate was 2 Hz. The image magnification was approximately 77 µm per pixel and the DIC pattern size was approximately 364 µm ($\approx$4.5 pixel), measured via the line intersection method. For data analysis, the chosen subset size was 21 pixel and the step size was 10 pixel to maximize the spatial resolution. This conforms with [11], which states the subset size should be at least three times the average DIC pattern size, and the step size a third to a half the subset size. The reference image was taken at a force tensile F = 0 kN while the specimen was only clamped by the top grip. For further analysis, the following coordinate system has been adopted: The abscissa was parallel to the specimen axis/loading direction (x axis in the Figures 3 and 4) and the ordinate was along the width of the specimen (y axis in Figures 3 and 4) with the origin being at the bottom centerline of the region of interest (ROI), see Figure 1 b). The postprocessed ROI does not cover the whole gauge section. Engineering strain was calculated using the commercial DIC software package.

RESULTS AND DISCUSSION

For the determination of the shear stress response using a coordinate transformation, a simplified equation (1) [15] has been used:

$$\tau = \sigma_{xx} \cdot \sin\varphi \cdot \cos\varphi, \tag{1}$$

with the shear stress, τ, being half the tensile stress (σ_{xx}) for loading angles φ of 45°. In practice, the nonuniformity in the tensile stress across the width of the specimen is usually ignored for the 10° specimens. The maximum shear strain, $\gamma_{12,max}$, has been calculated using the DIC-calculated principal strains ε_1 and ε_2:

$$\varepsilon_{12} = \frac{\varepsilon_1 - \varepsilon_2}{2} = \frac{1}{2}\gamma_{12,max} . \tag{2}$$

The resulting shear stress-shear strain curves are depicted in Figure 2 a). According to [4, 5, 7], the shear modulus for testing of composites should be extracted between a range of shear strain of $\gamma_{12} = (0.2 \text{ to } 0.6)\%$. Due to the non-flat character of the bias-extension specimen, an offset in shear strain occurred during full clamping of the specimen. Since the bias-extension specimen did not fracture (see Figure 2 b), no ultimate shear strength was extracted, therefore shear stress-strain curves were truncated at a shear strain of $\gamma_{12} = 6\% \pm 0.05\%$.
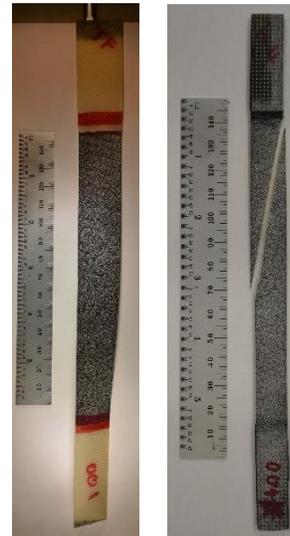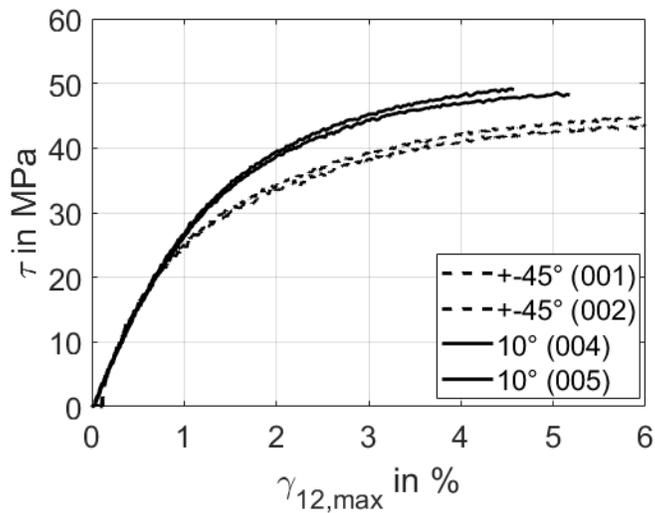
Figure 2: a) Shear stress-shear strain curves for two specimens each of ± 45° and 10°. The numbers in parenthesis indicate specimen number. Images of specimens post-tensile testing b) ± 45° c) 10°.

Figure 2 c) shows a representative specimen, loaded 10° counterclockwise from fiber orientation, that failed in the gauge section, close to the tabs. Measurements of the angle between fracture surface and edge of the specimen showed values in the nominal range of 9.9° ± 0.1°. Well-defined indentations in the tabs resulting from the diamond-wedge gripping show that no slipping occurred between tabs and grips.

We further utilize DIC analysis to understand the role of the initial out-of-plane deformation on the initial state of the specimen in the bias extension tests. Figure 3 shows the effect of the ± 45° non-planar through DIC analysis of out-of-plane deformation. Here W represents the displacement of the specimen surface in the z-axis (out of plane of page), with the z-origin defined as the surface with only the top clamp attached to the sample. Gripping the top and bottom of the specimen flattens the arched specimen at the ends and results in an out-of-plane displacement with an absolute value of approximately 2 mm. Conversely, the balanced lay-up of the 10° off-axis specimen exhibits limited out-of-plane deformation between full gripping and prior to final fracture in figure 3b.
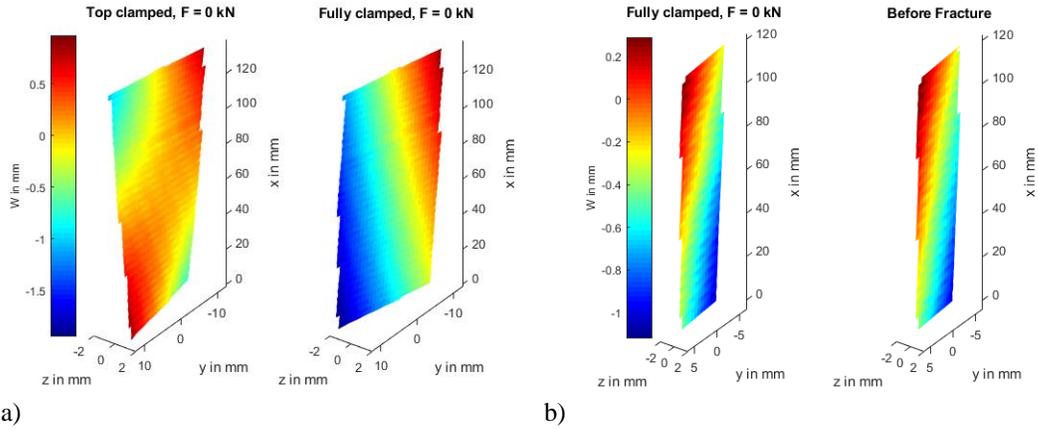
Figure 3: False color images of out-of-plane deformation for a) ± 45° and b) 10° (non-uniform coordinates).

The full strain field during tensile testing is visualized with DIC and this information allows for a rigorous analysis of the interaction between strain and the fiber orientation within the plaques. Figure 4 depicts iso-displacement contour plots in the axial (U, x) and lateral (V, y)) directions determined at an average shear strain in the elastic region of approximately $\gamma_{12} = 0.6$ %. The calculated axial displacements U show a nonuniformity with a gradient in the tensile direction of Figure 4a and 4b. Across the width of the specimen, the ± 45° specimen (Figure 4a) shows a uniform axial displacement. The 10° bias extension specimen (Figure 4b) exhibits nonuniformity across the width of the specimen due to the greater degree of extension-shear coupling.

A comparison to analytical solutions [10] for the calculation of the lateral displacements on the 10° specimen is provided in the right plot of Figure 4c. The analytical lateral displacement contours (right plot of Figure 4c)) show a nonuniformity over of the 10° specimen length and width, displaying an inverse 'S-shape' deformation.
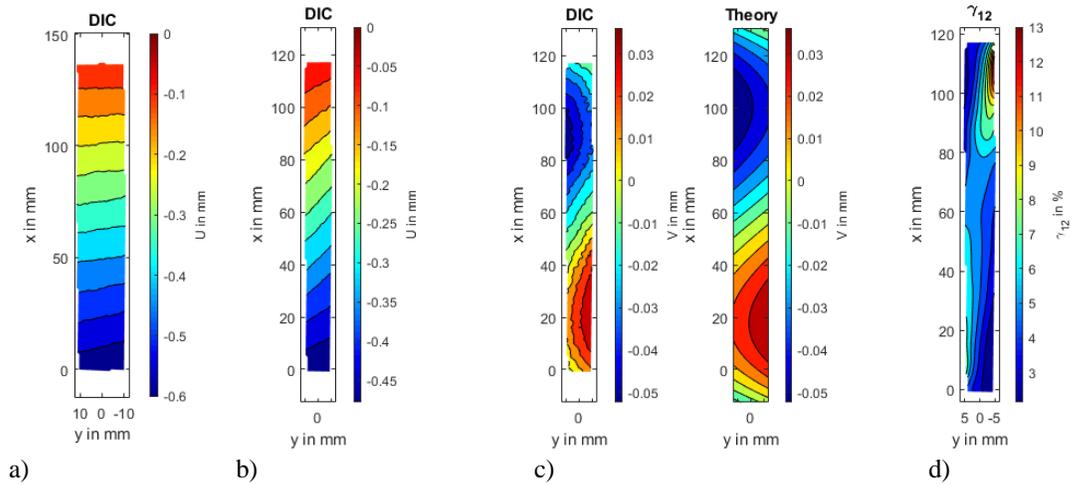
Figure 4: False color contour plots for axial displacement: a) ± 45° b) 10°, c) DIC-calculated and theoretical lateral displacement of 10°, d) shear strain on 10° just prior to failure.

Figure 4d) depicts the nonuniformity in the maximum shear strains (γ_{12}) prior to fracture of the 10° specimen. The gauge section shows an inhomogeneous strain distribution representing the complex biaxial strain state with a strain concentration in the upper corner of the specimen close to the upper grip. The highest values of γ_{12} are concentrated in this part of the specimen, where the fracture initiated across the specimen during failure.

CONCLUSIONS AND OUTLOOK

Figure 5 summarizes the shear properties for the epoxy based GFRP by comparing the types of tests discussed herein and the V-notch-rail testing of UD GFRP, presented in [13]. The values result from at least two specimens. In terms of the shear modulus (*G*), all shear tests investigated show comparable shear moduli. The ultimate shear strength (USS) was smaller for the 10° off-axis test compared to the V-notched rail test. The bias extension test (± 45°) does not result in a strength value, since the specimen did not fail. It should be noted that the V-notched-rail specimens exhibited a mixed mode (Modes I-III) character prior to failure, leading to inhomogeneous stress states within the gauge section. This is likely due to the thickness of the laminates ending up lower than recommended in the ASTM test method. The 10°-axis test measures strength values that are smaller than the V-notched-rail test, which likely result from strain concentrations near the clamping.
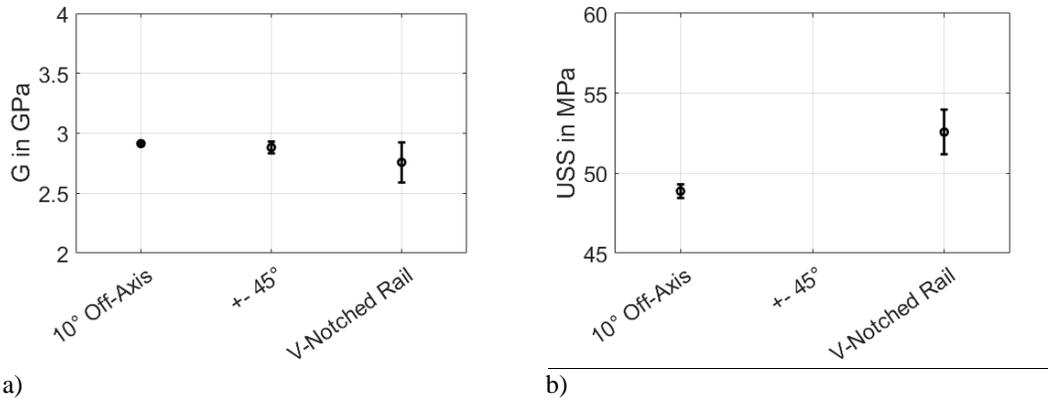
Figure 5: Comparison of the shear moduli a) and ultimate shear strength b) (average values and standard deviation from 2 tests per testing configuration) in comparison to the data from [13].

This work describes the use of DIC for measuring full-field surface displacements and strain response while performing bias-extension and 10° off-axis tensile tests on rigidly-clamped glass-fiber-reinforced coupon specimens. The advantage of using stereo DIC includes: mapping of the induced deformations and strains that reveal the phenomenology of deformation and damage throughout the specimen, which to date are difficult to observe using linear strain gauges or rosette strain gauges.

Future research will investigate the influence of the tab geometry for 10° off-axis specimens to reduce grip effects and the stress-strain response of symmetric ± 45° layups to achieve a USS value. An accurate strain transformation based on the normal strains and shear strain for an investigation of the strain perpendicular to the fiber direction could give insight into a possible failure mechanism during off-axis shear testing and loading under usage conditions or model validation. A detailed comparative study of different shear testing methods for the determination of the intra- and interlaminar properties, such as modulus and strength, of different fiber reinforced composites is being pursued.

ACKNOWLEDGMENTS

DISCLAIMER

Certain commercial equipment and/or materials are identified in this report in order to adequately specify the experimental procedure. In no case does such identification imply recommendation or endorsement by the National Institute of Standards and Technology, nor does it imply the equipment and/or materials used are necessarily the best available for the purpose.

REFERENCES

1. D2344/D2344M, A., *Short-Beam Strength of Polymer Matrix Composite Materials and Their Laminates.* 2016.
2. 08, A.D., *Standard Test Method for In-Plane Shear Strength of Reinforced Plastics.* 2015.
3. Merzkirch, M. and T. Foecke, *Investigation of the Interlaminar Shear Properties of CFRP via Flexural Testing using Digital Image Correlation.* Fatigue and Fracture Mechanics for Materials Performance and Characterization, 2019. **Submitted**.
4. *ASTM D5379/D5379M − Standard Test Method for Shear Properties of Composite Materials by the V-Notched Beam Method.* 2012, ASTM International: West Conshohocken, PA.
5. *ASTM D7078/D7078M − Standard Test Method for Shear Properties of Composite Materials by V-Notched Rail Shear Method.* 2012, ASTM International: West Conshohocken, PA.
6. Adams, D.F. *The Picture Frame Shear Test method.* 2014 10/31/2014 [cited 2019 6/11/]; Available from: https://www.compositesworld.com/articles/the-picture-frame-shear-test-method.
7. *ASTM D3518/D3518M − Standard Test Method for In-Plane Shear Response of Polymer Matrix Composite Materials by Tensile Test of a +-45° Laminate.* 2013, ASTM International: West Conshohocken, PA.
8. 14129, I., *ISO 14129 - Fibre-reinforced plastic composites - Determination of the in-plane shear stress/shear strain response, including the in-plane shear modulus and strength, by the plus or minus 45 degree tension test method.* 1998.
9. Chamis, C.C. and J.H. Sinclair, *Ten-deg off-axis test for shear properties in fiber composites.* Experimental Mechanics, 1977. **17**(9): p. 339-346.
10. Merzkirch, M. and T. Foecke. *10° Off-Axis Tensile Testing of Carbon Fiber Reinforced Polymers Using Digital Image Correlation.* in *Proceedings of Annual Conference and Exposition on Experimental and Applied Mechanics.* 2019. Reno, Nevada.
11. *International Digital Image Correlation Society - A Good Practices Guide for Digital Image Correlation*, E.M.C.a.I. Jones, M.A., Editor. 2018, International Digital Image Correlation Society iDICs.
12. An, Q., et al., *Tailored glass fiber interphases via electrophoretic deposition of carbon nanotubes: Fiber and interphase characterization.* Composites Science and Technology, 2018.
13. An, Q., M. Merzkirch, and F.A. M. *Characterizing Fiber Reinforced Polymer Composites Shear Behavior with Digital Image Correlation.* in *American Society for Composites - Thirty-third Technical Conference.* 2018. Seattle, Washington: Lancaster, PA, USA: DEStech Publications, Inc.
14. Merzkirch, M., *Mechanical Characterization using Digital Image Correlation: Advanced Fibrous Composite Laminates.* to be submitted.
15. Pindera, M.J. and C.T. Herakovich, *Shear Characterization of Unidirectional Composites with the Off-Axis Tension Test.* Experimental Mechanics, 1986. **26**(1): p. 103-112.